Interfacial Phenomena and Heat Transfer, 5(4):273–286 (2017)

CALCULATION OF BRIDGE SHAPE AND VELOCITY FIELD IN A GAP BETWEEN INCLINED CYLINDERS

Pavel I. Geshev

Kutateladze Institute of Thermophysics, Lavrentiev Ave. 1; Novosibirsk State University, Pirogova Str. 2, Novosibirsk, 630090, Russia; Tel.: +7 383 335 6057; Fax: +7 383 330 8480, E-mail: Geshev@itp.nsc.ru

Original Manuscript Submitted: 1/6/2018; Final Draft Received: 3/25/2018

A model of a liquid bridge that appears in a gap between two cylinders, inclined to the horizon, is developed. The shapes of the free surface of the bridges are calculated by the hydrostatic equations. The forces acting on the cylinders are determined. The velocity field in the current bridge flow is calculated by the method of boundary elements from the Navier–Stokes equation reduced to the Laplace equation. The volumetric flow rates of the liquid in the inclined bridge are calculated. For liquid flows in narrow gaps, an approximate model is constructed and the results are compared with the calculations obtained by the boundary element method.

KEY WORDS: *surface tension, contact angle, Laplace equation, Green function, boundary element*

1. INTRODUCTION

The motion of a liquid in a form of a bridge flowing in a gap between two inclined tubes is observed in different types of heat exchangers. This raises questions about the bridge shape, maximal amount of liquid held in it, volumetric flow rate of liquid in the bridge, its average velocity, and heat transfer through the bridge to the surrounding vapor. Studies on the shapes of two-dimensional drops suspended under a plane or rivulets on the bottom surface of the cylinder can be attributed to this theme, such as Buevich and Butkov (1969); Pitts (1973); Alekseenko et al. (1997); and Tanasijczuk et al. (2010). The determination of equilibrium shapes of liquid droplets and bridges is based on the hydrostatic equation, which is reduced to the nonlinear differential equation relative to the coordinates of the free surface. The nonlinear character of the problem requires the use of iterative methods, such as the Newton method. A general analytic representation for the coordinates of a free surface of a two-dimensional drop through elliptic integrals was obtained by Pitts (1973). The curvature at the lower point of the drop was the preset parameter. Here, we do not use the Pitts (1973) solution. Our approach is based on direct calculation of the coordinate of the upper contact point by the Newton method from some non-linear integral equation.

In the literature, we have found only three publications related directly to the bridges. These are the works of researchers at the Kutateladze Institute of Thermophysics: Alekseenko and Kuibin (1996); Maltsev and Zuikova (2004); and Maltsev et al. (2016). In Alekseenko and Kuibin (1996), they considered only a case with a zero contact angle. In Maltsev and Zuikova (2004) and Maltsev et al. (2016), they used an iterative method, which in contrast to the Newton universal method for solving nonlinear problems, gave limited possibilities for finding solutions. In this work, we continue the studies started in the aforementioned research studies, and we additionally investigate the forces acting on the cylinders and calculate the velocity fields and volumetric flow rates of liquid in the bridges between inclined tubes by the method of boundary integral equations.

Let us consider a liquid bridge held by the capillary force between two cylinders with radius R. The cylinders are located in a vertical plane with distance D between them and angle of inclination to the horizon γ. We direct the Y-axis down along the symmetry line connecting the centers of cylinders (Fig. 1). The X-axis is directed perpendicular to the vertical plane and Z-axis is directed along the cylinders. A gravity component with acceleration $g_z = g\sin\gamma$, leading to a laminar liquid flow with velocity $W(X, Y)$, acts along the Z-axis. The shape of the bridge does not

2169–2785/17/$35.00

NOMENCLATURE

D	gap between two cylinders, dimensional (m)
g	acceleration of gravity, dimensional (m/s^2)
H	vertical length of the bridge, dimensional (m)
K	local curvature of the free surface, dimensional (m^{-1})
P_{atm}	pressure in gas around the bridge, dimensional (N/m^2)
P_α	pressure in the bridge at the lower contact point, dimensional (N/m^2)
P_β	pressure inside the bridge at the upper contact point, dimensional (N/m^2)
Q	liquid flow rate in the bridge, dimensional (m^3/sec)
R	radius of the cylinder, dimensional (m)
S	cross-sectional area of the bridge, dimensional (m^2)
W	liquid velocity of the bridge flow (Q/S), dimensional (m/s)
W^*	characteristic velocity of liquid, dimensional (m/s)
X, Y, Z	Cartesian coordinates, dimensional (m)

Dimensionless Quantities

A	maximal area of the bridge, dimensionless
Bo	Bond number, $\rho g R^2/\sigma$
d	gap between two cylinders, D/Λ
G	Green function
h	vertical distance between the upper and lower contact points, H/Λ
q	liquid flow rate
s	dimensionless area of the bridge cross section, S/Λ^2
x, y, z, r	dimensionless coordinates and radius: X/Λ, Y/Λ, Z/Λ, R/Λ
$\vec{x}$	integration point vector [$= (x, y)$]
$\vec{\xi}$	observation point vector [$= (\xi, \eta)$]

Greek Symbols

α	central angle at the lower contact point (°, rad)
β	central angle at the contact point on the upper cylinder (rad)
γ	tilt angle of tubes (°)
Δ	x-coordinate of the bridge surface, dimensional (m)
δ	x-coordinate of the bridge surface, dimensionless
δ_D	Dirac's δ function, dimensionless
θ	contact wetting angle (°)
κ_α, κ_β	dimensionless curvatures at the upper and lower points
Λ	Laplace scale or capillary length, dimensional (m)
ν	kinematic viscosity of liquid, dimensional (m^2/s)
ρ	liquid density, dimensional (kg/m^3)
σ	surface tension, dimensional (N/m)
ϕ	angle between the tangent to the free surface and axis Y (rad)

change along the Z-axis and does not depend on velocity $W(X, Y)$; the shape is determined by the hydrostatic equation in the X and Y coordinates. After determining the bridge shape, it is possible to calculate the forces acting on the cylinders, bridge area, velocity field, and volumetric flow rate of the liquid in the bridge.

The bridge shapes can be different. They are determined by dimensionless parameters: cylinder radius r, contact angle θ, and inter-tubular distance d. To obtain an unambiguous solution, we should also specify angle α of the contact point of the free surface on the lower cylinder. There are four independent parameters (r, θ, d, and α) that determine the solution to the bridge problem, i.e., we have a very rich four-dimensional parametric space. In the subsequent sections, examples of bridges and their areas, flow rates, and fluid velocities as functions of parameters α and d for some fixed cylinder radii r and contact angles θ are calculated.

In Section 2, we derive the basic equation determining the bridge shape and formulate an inequality for the parameters of the problem that bounds the region of existence for the solutions in the parametric space. In Section 3,

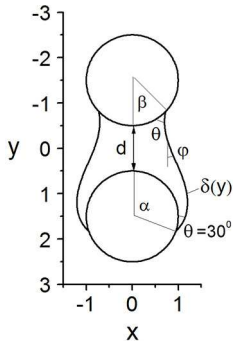

FIG. 1: Example of calculated liquid bridge between the cylinders with dimensionless radii $r = 1$, inter-tubular distance $d = 1$, and contact angle $\theta = 30°$, relevant for water/aluminum [angles α and β determine the position of the contact points (for this example, $\alpha = 108.9°$ and $\beta = 46.7°$); φ is the angle between the free surface of the liquid at any point and axis y; $\delta(y)$ is the x-coordinate of the free surface]

the formulas for the forces acting on the cylinders are derived. Section 4 describes the algorithm for calculating the two-dimensional velocity field and liquid flow rates in bridges of water and Freon 21. In Section 5, the main conclusions are formulated.

2. CALCULATION OF BRIDGE SHAPE

The pressure under the curved free surface of liquid (P_s) is determined by its local curvature K using the classic formulas of the Laplace–Young theory (Landau and Lifshits, 1987):

$$\begin{aligned} P_s &= P_{\text{atm}} - \sigma\, K \\ K &= \frac{\Delta''}{\left(1+\Delta'^2\right)^{3/2}} \end{aligned} \tag{1}$$

where σ is the surface tension coefficient for liquid; P_{atm} is the atmospheric pressure of the ambient gas; and Δ is the coordinate of the free surface (or local semi-width of the bridge), in which the prime and double prime indicate the derivative with respect to coordinate Y. From the equation of hydrostatics, $\nabla P = \rho\vec{g}$ (Landau and Lifshits, 1987), after integrating along the Y-axis, we obtain the pressure at any point of Y near the curved free surface

$$P_s = P_\beta + \rho g_y \left(Y - Y_\beta\right) \tag{2}$$

where P_β is the liquid pressure at the upper contact point of the free surface; β is the angle of the contact point position relative to the Y-axis; Y_β is the coordinate of the upper contact point; ρ is the liquid density; and $g_y = g\cos\gamma$ is the gravity acceleration along the y-axis. We exclude P_s from Eqs. (1) and (2) and obtain

$$\frac{\sigma\Delta''}{\left(1+\Delta'^2\right)^{3/2}} = \left(P_{\text{atm}} - P_\beta\right) - \rho g_y \left(Y - Y_\beta\right) \tag{3}$$

Differential Eq. (3) describes the local curvature, which varies along the free surface. At the contact points, this surface must approach the surface of the cylinders at a certain contact angle θ. The conditions at the contact points are two necessary boundary conditions to second-order Eq. (3).

Let us introduce the dimensionless values: two coordinates, the radius of the cylinder, and the x-coordinate of the bridge surface

$$x = \frac{X}{\Lambda}, \quad y = \frac{Y}{\Lambda}, \quad r = \frac{R}{\Lambda}, \quad \delta = \frac{\Delta}{\Lambda}$$

where $\Lambda = \sqrt{\sigma/\rho g_y}$ is the characteristic Laplace scale. Let us introduce the value $\kappa_\beta = [(P_{\text{atm}} - P_\beta)/\sigma]\,\Lambda$, which is the dimensionless curvature of the free surface at upper point Y_β. A similar curvature, $\kappa_\alpha = [(P_{\text{atm}} - P_\alpha)/\sigma]\,\Lambda$, is introduced for lower contact point Y_α. It is convenient to set the contact points by angles α and β as shown in Fig. 1

$$x_\alpha = r\sin\alpha \tag{4}$$

$$x_\beta = r\sin\beta \tag{5}$$

$$y_\alpha = \frac{d}{2} + r\,(1-\cos\alpha) \tag{6}$$

$$y_\beta = -\frac{d}{2} - r\,(1-\cos\beta) \tag{7}$$

where d is the dimensionless gap between cylinders. Let us note that the square of the dimensionless radius defines Bond number $\text{Bo} = \rho g R^2/\sigma = r^2$, which is the relative measure for the effect of gravitational forces. There are many works on fluid capillary structures at zero or very small Bond numbers (see, for example, Myshkis, 1976; Kralchevsky and Nagayama, 2001; Reyssat, 2015). However, in our work, very interesting shapes of the free surface arise at larger Bo numbers. Therefore, we do not impose any restrictions on the Bond number.

We will use free surface height $h = (y_\alpha - y_\beta)$, for which the following expression is derived from formulas (6) and (7)

$$h = d + 2r\left[\sin^2(\alpha/2) + \sin^2(\beta/2)\right] \tag{8}$$

We integrate Eq. (3) from y_β to y and obtain the following dimensionless expression:

$$\sin\phi = \frac{\delta'}{\sqrt{1+\delta'^2}} = \kappa_\beta\,(y-y_\beta) - \frac{(y-y_\beta)^2}{2} + \sin\phi_\beta \tag{9}$$

where ϕ_β and ϕ are the angles between the y-axis and free surface of liquid at points y_β and y, respectively (Fig. 1). At the lower contact point, Eq. (9) gives $\sin\phi_\alpha$. As a result, we obtain equation

$$\sin\phi_\alpha - \sin\phi_\beta = \kappa_\beta\,(y_\alpha - y_\beta) - \frac{(y_\alpha - y_\beta)^2}{2} \tag{10}$$

where angles α, ϕ_α, β, and ϕ_β are connected with contact angle θ through the relationships

$$\phi_\alpha = \pi/2 - (\alpha+\theta) \tag{11}$$

$$\phi_\beta = (\beta+\theta) - \pi/2 \tag{12}$$

The relationship for surface curvature at upper point κ_β follows from formula (10):

$$\kappa_\beta = \frac{\cos(\alpha+\theta) + \cos(\beta+\theta)}{h} + \frac{h}{2} \tag{13}$$

According to Eq. (3), the dimensionless surface curvature at lower point y_α is

$$\kappa_\alpha = \kappa_\beta - h = \frac{\cos(\alpha+\theta) + \cos(\beta+\theta)}{h} - \frac{h}{2} \tag{14}$$

This curvature is smaller than that at κ_β, and at high values of h it can be negative, which according to Eq. (1) will cause an increase in the pressure at lower contact point y_α.

Using relations (11) and (12), from Eq. (9) we obtain the differential equation describing the free surface of liquid:

$$\frac{\delta'}{\sqrt{1+\delta'^2}} = \frac{(y-y_\beta)\cos(\alpha+\theta) + (y-y_\alpha)\cos(\beta+\theta)}{h} + \frac{(y_\alpha - y)(y-y_\beta)}{2} \tag{15}$$

Representing the right-hand side of Eq. (15) through $\sin\phi\,(y)$, after its integration we obtain

$$\delta = x_\beta + \int\limits_{y_\beta}^{y} \frac{\sin\phi\,(y)\,dy}{\sqrt{1-\sin^2\phi\,(y)}} \tag{16}$$

The complete integral gives an additional equation, connecting unknown values

$$x_\alpha - x_\beta = \int\limits_{y_\beta}^{y_\alpha} \frac{\sin\phi\,(y)\,dy}{\sqrt{1-\sin^2\phi\,(y)}} \tag{17}$$

where all coordinates of the contact points are determined by formulas (4)–(7).

Equation (17) connects two angular coordinates of contact points α and β with the problem parameters: contact angle θ, distance d, and cylinder radius r. Setting angle α and solving Eq. (17) by the Newton method we obtain the second angle β as a function of α and the previously listed parameters. Using the calculated value $\beta(\alpha)$, we can calculate the free surface by Eq. (16).

Upper contact angle $\beta(\alpha)$ was calculated for increasing values of angle α, as shown in Fig. 2 for $r = 1$, $\theta = 30°$, and $d = 1$. This contact angle is characteristic for the case of a water bridge confined between aluminum tubes. One can see that angle β increases to a certain maximum, and then begins to decrease [Fig. 3(a)]. The cross-sectional area of bridge [Fig. 3(b)] also can go through the maximum, but the maximum is placed at other values of angle α. The maximum of the bridge area is an important characteristic since it determines the bearing capacity of the bridge. We calculated this maximum of the bridge area ($A = s_{\max}$); the dependence of this value on the parameters of the problem is shown in Fig. 4 for four contact angles. It is obvious that with increasing contact angle θ, the region of distances d, where the solutions are still found by the Newton method, is compressed.

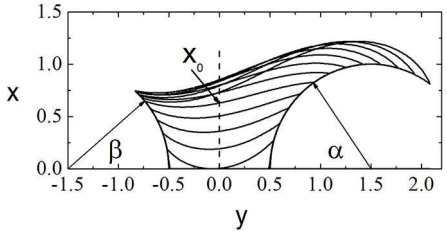

FIG. 2: For the given parameters of the problem ($r = 1$, $d = 1$, and $\theta = 30°$) and for some values of α, the angle $\beta(\alpha)$ is calculated and corresponding free surfaces $\delta(y)$ are shown

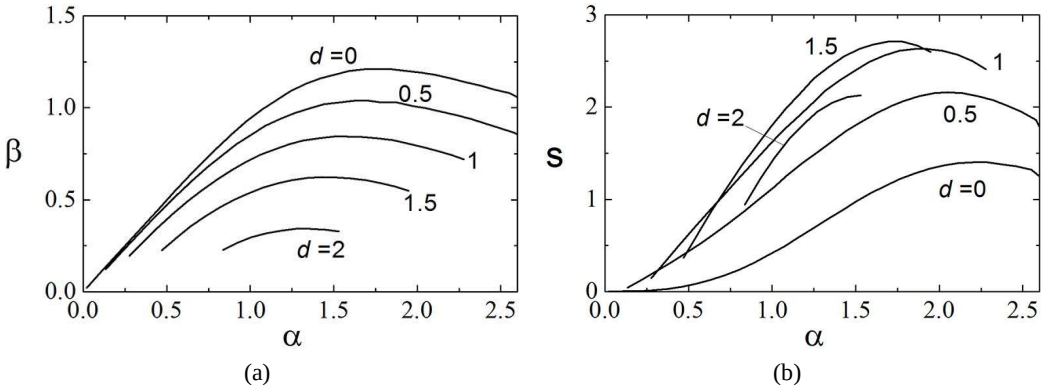

FIG. 3: (a) Angles $\beta(\alpha)$ and (b) areas $s(\alpha)$ of the bridge cross section are calculated for five different gaps d and for the parameters as in Figs. 1 and 2: $r = 1$ and $\theta = 30°$

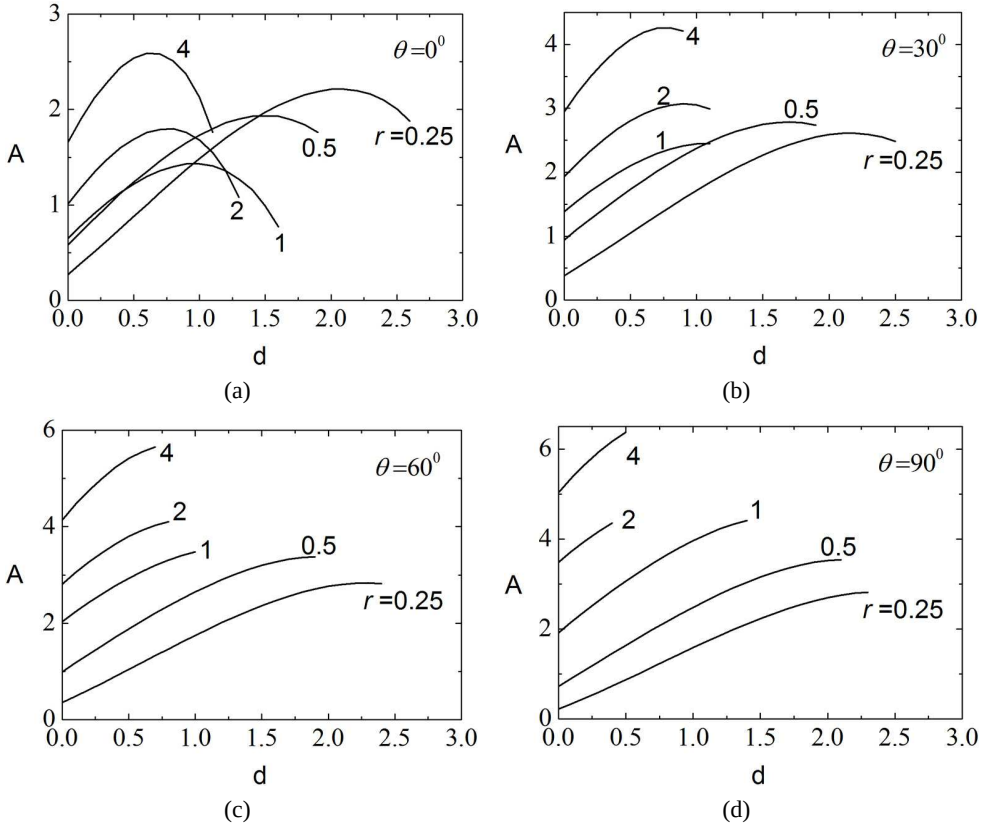

FIG. 4: Maximal bridge area A versus distance $d$for five values of radius r (0.25, 0.5, 1, 2, and 4) and four contact angles θ: (a) 0°; (b) 30°; (c) 60°; (d) 90°

Various shapes of calculated bridges with maximal cross-sectional area A are shown in Fig. 5 for two values of the cylinder radius, two contact angles, and several distances d. For small cylinder radii [Fig. 5(a), $r = 0.5$] distance d can be quite large ($d = 2$). For large cylinder radii [Fig. 5(b), $r = 2$] and contact angle $\theta = 90°$ the value of d, at which the solutions are still found by the described method, decreases and becomes less than 0.5.

According to the denominator in integral Eq. (17), the following inequality must be fulfilled for the sine at all coordinates y:

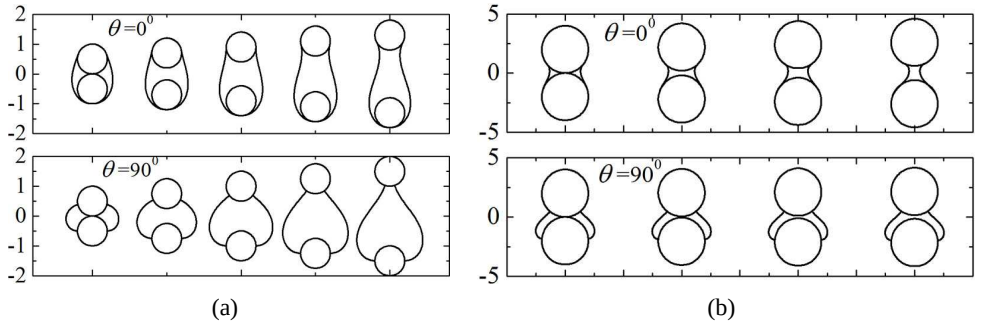

FIG. 5: Version of bridge shapes for two contact angles (0° and 90°), two cylinder radii [(a) $r = 0.5$; (b) $r = 2$], and different distances d (bridges of the maximal area are presented)

$$\sin\phi(y)=\frac{(y-y_\beta)\cos(\alpha+\theta)+(y-y_\alpha)\cos(\beta+\theta)}{h}+\frac{(y_\alpha-y)(y-y_\beta)}{2}<1$$

From this equation, we derive the important inequality

$$h=d+2r\left[\sin^2(\alpha/2)+\sin^2(\beta/2)\right]<2\left[\sin\left(\frac{\alpha+\theta}{2}\right)+\cos\left(\frac{\beta+\theta}{2}\right)\right] \tag{18}$$

which sets the limiting boundaries for the parameters in the four-dimensional parametric space. Here, upper contact angle β is the solution to Eq. (17) and it depends on the other four independent parameters: α, d, r, and θ. We see that according to inequality (18) parameters r and d cannot be arbitrarily large (in any case, h and d should be less than 4), and for large radius r angles α and β should be small.

3. FORCES ACTING ON THE CYLINDERS

The force acting on the cylinder consists of the pressure force determined by the integral over the wetted surface and surface tension forces applied at the contact points. Dimensionless pressures on the surface of the lower (p_α) and upper (p_β) cylinders can be written in the following form:

$$\begin{aligned}p_\alpha&=(y-y_\alpha)-\kappa_\alpha\\ p_\beta&=(y-y_\beta)-\kappa_\beta\end{aligned} \tag{19}$$

where curvatures κ_β and κ_α are set by formulas (13) and (14). We integrate the pressure over the wetted surfaces of the cylinders and add the surface tension forces to these integrals. We obtain the following formulas for the forces acting on the lower and upper cylinders:

$$f_\alpha=-2\kappa_\alpha r\sin\alpha-r^2(\alpha-\sin\alpha\cos\alpha)-2\cos\phi_\alpha \tag{20}$$

$$f_\beta=2\kappa_\beta r\sin\beta-r^2(\beta-\sin\beta\cos\beta)+2\cos\phi_\beta \tag{21}$$

When substituting relationships (13) and (14), we obtain the forces acting on the lower and upper cylinders, respectively:

$$f_\alpha=-2r\sin\alpha\left(\frac{\sin(\alpha+\theta)+\sin(\beta+\theta)}{h}-\frac{h}{2}\right)-r^2(\alpha-\sin\alpha\cos\alpha)-2\sin(\alpha+\theta) \tag{22}$$

$$f_\beta=2r\sin\beta\left(\frac{\sin(\alpha+\theta)+\sin(\beta+\theta)}{h}+\frac{h}{2}\right)-r^2(\beta-\sin\beta\cos\beta)+2\sin(\beta+\theta) \tag{23}$$

The forces are the functions of the two angles (α and β) and three parameters of the problem (d, r, and θ). The sum of forces should equal the bridge weight, and this gives the following formula for the dimensionless area of the bridge:

$$s=f_\alpha+f_\beta \tag{24}$$

The validity of this expression can be checked by direct calculation of the bridge area via the integration of the local bridge width (2δ) and subtraction of the areas of two cylindrical segments:

$$s=2\int_{y_\alpha}^{y_\beta}\delta(y)\,dy-(\alpha-\cos\alpha\sin\alpha)r^2-(\beta-\cos\beta\sin\beta)r^2 \tag{25}$$

Figures 6 and 7 show the forces acting on the lower (f_α) and upper (f_β) cylinders and the maximal bridge area ($A=s_{\max}$), depending on the width of inter-tubular gap d for two contact angles and three cylinder radii. The forces and bridge area are calculated via expressions (22), (23), and (25), and equality (24) is fulfilled with high accuracy. The maximal relative difference between the two calculated bridge areas [Eqs. (24) and (25)] is less than 10^{-4}. This accuracy corresponds to the number of control points ($N=200$) taken on free surface Σ in our calculations.

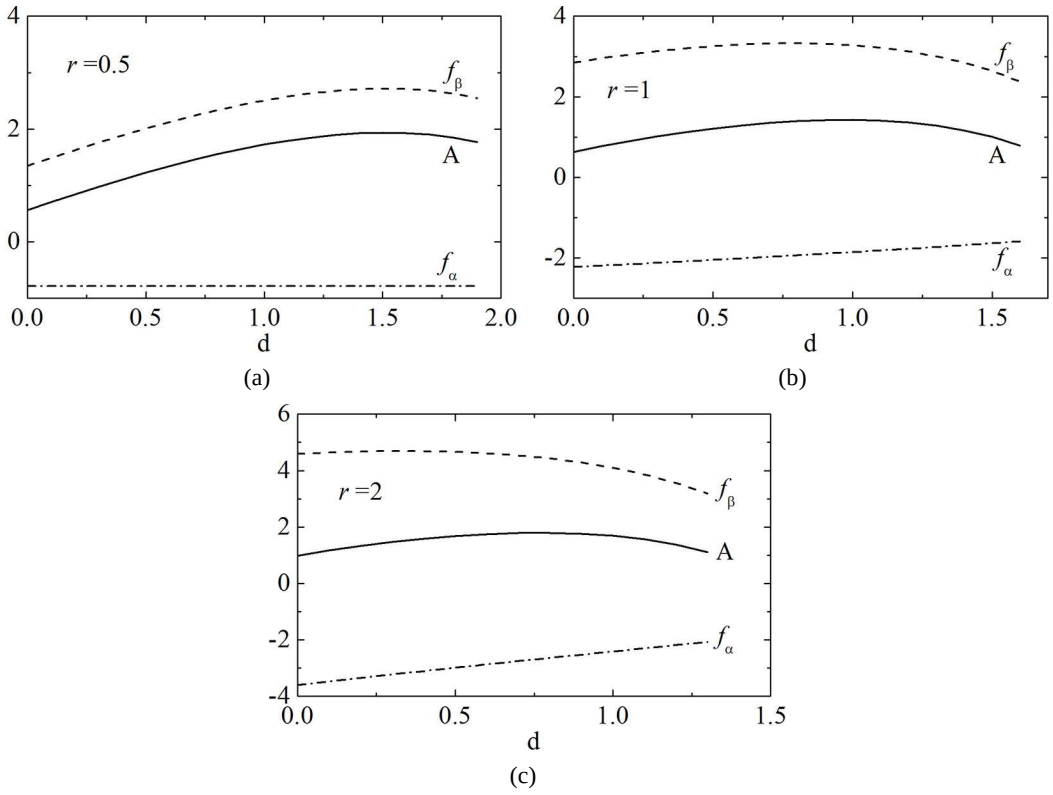

FIG. 6: Forces acting on lower (f_α) and upper (f_β) cylinders versus d for three values of cylinder radii [(a) $r = 0.5$; (b) $r = 1$; (c) $r = 2$], and contact angle $\theta = 0°$ [forces are calculated by formulas (22) and (23) and their sum coincides with area (A), calculated via integration of the coordinates of the free surface; bridges of maximal area A are considered]

We should note that the force acting on the lower cylinder (f_α) for the zero contact angle (Fig. 6) is always negative. This is because the rarefied pressure in the bridge pulls the lower cylinder upward. For contact angle $\theta = 90°$ (Fig. 7), force f_α is always positive (directed downward), and force f_β can be negative (directed upward for small d) and positive, and even at certain distances d this force can become greater than force f_α. This can be explained by the increased pressure in the bridge, which has a convex free surface at $\theta = 90°$ (Fig. 5).

4. LAMINAR FLOW OF LIQUID IN THE BRIDGE

For velocity component W, longitudinal along axis Z, we have the equation

$$\nu\left(\frac{\partial^2}{\partial X^2}+\frac{\partial^2}{\partial Y^2}\right)W=-g\sin\gamma \tag{26}$$

where ν is the kinematic viscosity, and γ is the angle of tube inclination relative to the horizon. We complete Eq. (26) with the zero boundary conditions: $W = 0$ (on the tube surface) and $\partial W/\partial n = 0$ (on the symmetry axis and free surface of the liquid). All coordinates are reduced to capillary scale $\Lambda = \sqrt{\sigma/\rho g\cos\gamma}$, and the velocity is reduced to the dimensionless form by characteristic value $W_* = (\sigma\sin\gamma)/(\eta\cos\gamma)$. For the dimensionless velocity, we derive the Poisson equation

$$\left(\frac{\partial^2}{\partial x^2}+\frac{\partial^2}{\partial y^2}\right)w=-1 \tag{27}$$

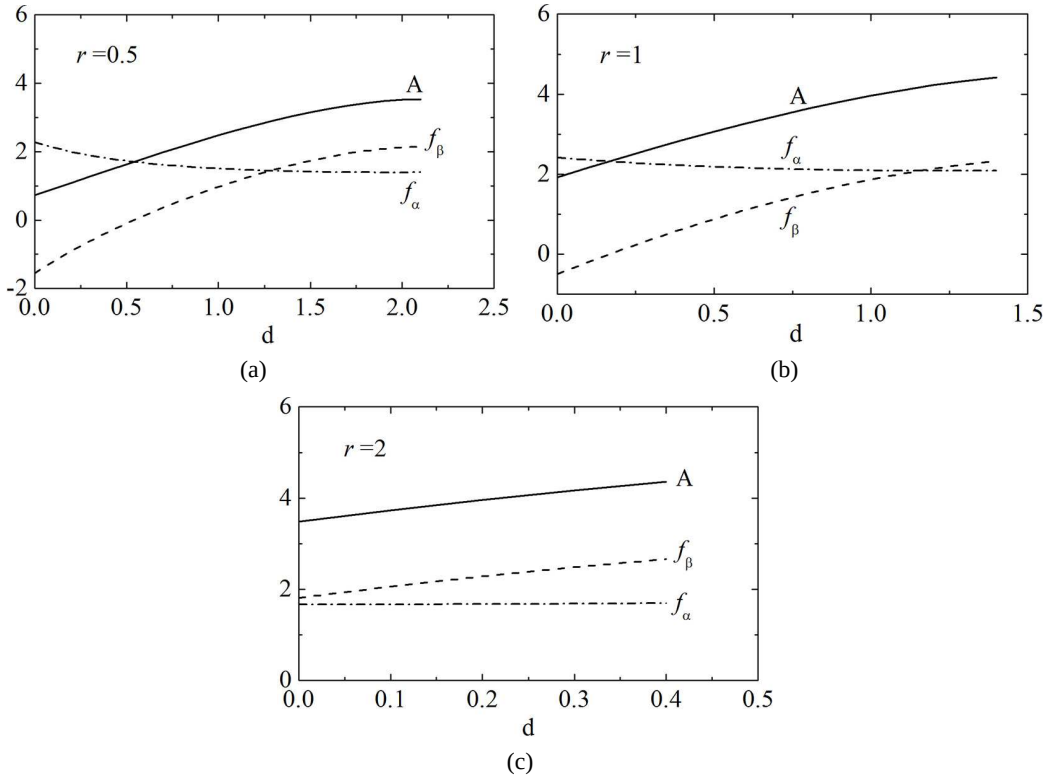

FIG. 7: Forces acting on lower (f_α) and upper (f_β) cylinders versus d for three cylinder radii [(a) $r = 0.5$; (b) $r = 1$; (c) $r = 2$] and contact angle $\theta = 90°$

To solve Eq. (27), the velocity field is presented as sum $w = v + \psi$, where v is the general solution to homogeneous Eq. (27) and $\psi = -(1/4) \cdot \left(x^2 + y^2\right)$ is the partial solution to non-homogeneous Eq. (27). Function v satisfies the Laplace equation

$$\left(\frac{\partial^2}{\partial x^2} + \frac{\partial^2}{\partial y^2}\right) v = 0 \tag{28}$$

Let us introduce the Green function of the Laplace equation

$$G = \frac{1}{2\pi} \ln \frac{1}{\left|\vec{x} - \vec{\xi}\right|}$$

satisfying the equation

$$\left(\frac{\partial^2}{\partial x^2} + \frac{\partial^2}{\partial y^2}\right) G = -\delta_D \left(\vec{x} - \vec{\xi}\right) \tag{29}$$

where Dirac's δ-function is used with vector arguments $\vec{x} = (x, y)$ and $\vec{\xi} = (\xi, \eta)$. We apply the Green theorem to Eqs. (28) and (29) and obtain value v at the inner points of the bridge by the Green formula

$$v\left(\vec{\xi}\right) = \oint_\Gamma \left[G\left(\vec{\xi} - \vec{x}\right) \frac{\partial v\left(\vec{x}\right)}{\partial n_x} - v\left(\vec{x}\right) \frac{\partial G\left(\vec{\xi} - \vec{x}\right)}{\partial n_x} \right] dl_x \tag{30}$$

where Γ is the bridge contour; coordinates $\vec{\xi}$ (observation points) are placed within the contour; and coordinates $\vec{x}$ (integration points) are laying on the contour. When approaching the observation point to contour Γ, we obtain in the

limit the boundary integral equation (Brebbia et al., 1984):

$$\frac{1}{2}v\left(\vec{\xi}\right)=\oint\limits_{\Gamma}\left[\mathrm{G}\left(\vec{\xi}-\vec{x}\right)\frac{\partial v\left(\vec{x}\right)}{\partial n_x}-v\left(\vec{x}\right)\frac{\partial \mathrm{G}\left(\vec{\xi}-\vec{x}\right)}{\partial n_x}\right]dl_x \tag{31}$$

The second term in singular integral (30) describes the potential of the double layer, which experiences a jump as observation point $\vec{\xi}$ passes through surface Γ. The magnitude of discontinuity, as is shown in the theory of integral equations, is equal to $v(\vec{\xi})$ (Brebbia et al., 1984). If point $\vec{\xi}$ lies exactly on surface Γ, then one-half of the jump in the second term of the integral is equal to $0.5v(\vec{\xi})$, and this value is subtracted from function $v(\vec{\xi})$ in Eq. (30), giving the term $0.5v(\vec{\xi})$ on the left-hand side in Eq. (31).

From the boundary conditions for velocity w and its normal derivative, we obtain the boundary conditions on the cylinder surfaces (C) and on the free surface of the liquid (Σ), respectively,

$$v|_C=-\psi|_C\,,\quad \left.\frac{\partial v}{\partial n}\right|_{\Sigma}=-\left.\frac{\partial \psi}{\partial n}\right|_{\Sigma} \tag{32}$$

These quantities are substituted into integral Eq. (31), and the unknown values of normal derivative $\partial v/\partial n$ on the cylinder surfaces (C) and function v itself on the free surfaces of liquid (Σ) are determined from the system of linear equations. We obtain this system of equations by dividing contour Γ into N small linear segments and integrating integral (31) over them. During the integration, the unknown values are considered as the constants along the elements. The integrals of function G and its normal derivative can be calculated analytically. The system of equations is solved by the Gauss method with a choice of a pivoting element. Actually, we have briefly described the method of constant boundary elements (Brebbia et al., 1984), which belongs to a class of direct (not iterative) methods of the solution to the elliptic problems of a potential theory and allows efficient calculation of the laminar flows with curvilinear free boundaries. Equation (31) is the basic boundary integral equation in the boundary element method (BEM) (see Brebbia et al., 1984).

The values of function $v(\vec{\xi})$ at the internal points of the bridge are determined by formula (30), where the boundary values v and their normal derivative are already known from the previous step. Based on the calculated velocity inside the bridge, we can calculate volumetric flow rate q and then the average liquid velocity

$$\bar{w}=q/s \tag{33}$$

where s is the cross-sectional area of the bridge by the plane perpendicular to the z-axis. However, it is possible to avoid calculating the two-dimensional integral in Eq. (33) by applying Green's theorem to two equations (Alekseenko et al., 1997):

$$\left(\frac{\partial^2}{\partial x^2}+\frac{\partial^2}{\partial y^2}\right)w=-1,\quad \left(\frac{\partial^2}{\partial x^2}+\frac{\partial^2}{\partial y^2}\right)\psi=-1 \tag{34}$$

and obtaining representation

$$q=\iint\limits_{s}w\left(x,y\right)dxdy=\oint\limits_{\Gamma}\left[\psi\left(\vec{x}\right)\frac{\partial w\left(\vec{x}\right)}{\partial n_x}-w\left(\vec{x}\right)\frac{\partial \psi\left(\vec{x}\right)}{\partial n_x}\right]dl_x+\iint\limits_{s}\psi\left(x,y\right)dxdy \tag{35}$$

where, using the specific properties of function ψ, the last two-dimensional integral can be transformed into the contour integral. First, we present function ψ as a divergence in the following form:

$$\psi=-\frac{1}{4}\left(x^2+y^2\right)=-\frac{1}{16}\mathrm{div}\left[\left(x^2+y^2\right)\vec{x}\right]$$

Then, we transform the double integral in Eq. (35) to the contour integral due to the Gauss theorem. As a result, we get a formula convenient for calculating the volumetric liquid flow rate:

$$q=\iint\limits_{s}w\left(x,y\right)dxdy=\oint\limits_{\Gamma}\left[\psi\left(\vec{x}\right)\frac{\partial w\left(\vec{x}\right)}{\partial n_x}-w\left(\vec{x}\right)\frac{\partial \psi\left(\vec{x}\right)}{\partial n_x}-\frac{1}{2}\psi\left(\vec{x}\right)\frac{\partial \psi\left(\vec{x}\right)}{\partial n_x}\right]dl_x \tag{36}$$

where all values on contour Γ are already known.

To demonstrate the flow rates and averaged velocities of the liquid in the bridges, we take two liquids: water and Freon R21 at temperatures 20°C and 40°C, respectively. The physical properties of the liquids are given in Table 1. The contact angles are found for water/steel, water/aluminum, and Freon/aluminum combinations. The surface tension for pure water is close to 0.07 N/m. With the addition of a surfactant, for example, surfynol, coefficient σ can be significantly reduced and may reach a value of 0.03 N/m. The cylinder radius is $R = 5$ mm; the size of the inter-tubular gap takes three values $D = 2.5$, 1.5, and 0.5 mm; and the angle of tube inclination is $\gamma = 7°$. To fix the free surface of the bridge, we can use a specific size, the half-width of the bridge (X_0), instead of angle α. This is measured from the symmetry line exactly along axis X (at $Y = 0$), as is shown in Fig. 2 by the dashed line. The dependences of the water flow rates on X_0 are shown in Fig. 8(a) and the average liquid velocities in the water bridges are shown in Fig. 8(b); the calculated values are shown by solid lines for θ = 60° and by dashed curves for θ = 30°. It can be seen that contact angle θ and surface tension σ can influence the maximal half-width of the bridge but affect insignificantly the behavior of curves $Q(X_0)$ at small X_0. Here, all curves for the same inter-tube distance D merge. The same can be said about the dependence of the average liquid velocity on the half-width of bridge (X_0) shown in Fig. 8(b); here, the dashed curves (θ = 30°) deviate insignificantly from the solid lines (θ = 60°).

Figures 9(a) and 9(b) show the flow rates and average velocities for the bridges of Freon. We should note that the maximal size of the Freon bridges ($X_{0,\max} \approx 0.5$–2.2 mm) are much less than those for water ($X_{0,\max} \approx 3.8$–4.4 mm). This is obviously caused by the small value of coefficient σ for Freon. However, due to the low viscosity of Freon and its higher density, flow rates Q and average liquid velocities W in the Freon bridges are significantly higher than those for water.

It is important to compare our calculations with the results obtained in the Maltsev et al. (2016), who used parameters θ = 36°, Bo = 13.48, and $D/R = 0.2$, which correspond to our parameters: $r = \sqrt{\text{Bo}} = 3.67$, $d = 0.2$, and $r = 0.734$. In Fig. 10, two of our calculated profiles of the bridges [Fig. 10(a)] and bridge area [Fig. 10(b)] are shown by solid curves, and comparisons with the data taken from Maltsev et al. (2016) are shown by black squares. One can see that the deviations between these two sets of data are very small, and therefore the two different methods used for the calculations are both exact and reliable.

TABLE 1: Physical properties of the liquids

Liquid/Solid	θ (°)	σ (N/m)	ρ (kg/m^3)	ν (m^2/s)	T (°C)	P_{atm}
Water/steel	60	0.07, 0.05, 0.03	1000	10^{-6}	20	1
Water/Al	30	0.07, 0.05, 0.03	1000	10^{-6}	20	1
Freon R21/Al	20	0.016	1330	0.2×10^{-6}	40	3

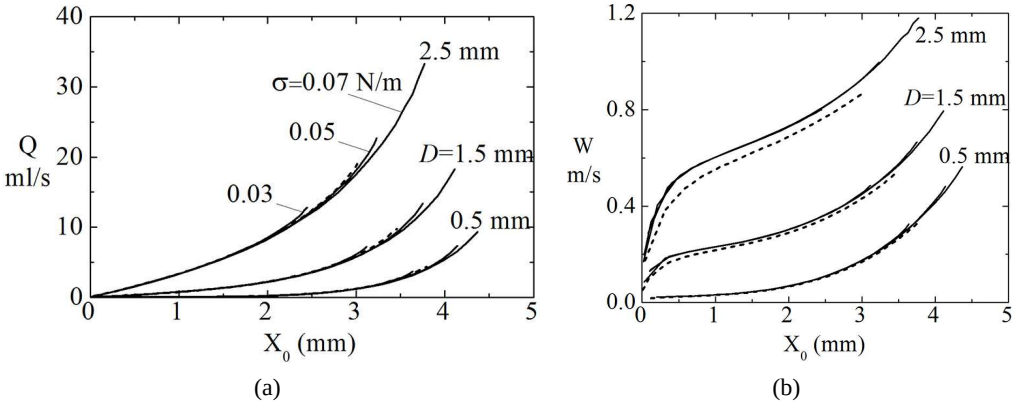

FIG. 8: (a) Water flow rates Q (in ml/sec) versus half-width of bridge X_0 (in mm) [parameters: inclination angle $\gamma = 7°$; inter-tube distances $D = 0.5$, 1.5, and 2.5 mm; cylinder radius $R = 5$ mm; contact angles θ = 60° (solid lines) and θ = 30° (dashed curves); coefficient σ = 0.07, 0.05, and 0.03 N/m]; (b) averaged water velocities W (m/sec) versus X_0 (mm) for the same solutions as in (a) (parameters $\gamma = 7°$; $D = 0.5$, 1.5, and 2.5 mm; $R = 5$ mm; θ = 60° and 30°; σ = 0.07, 0.05, and 0.03 N/m)

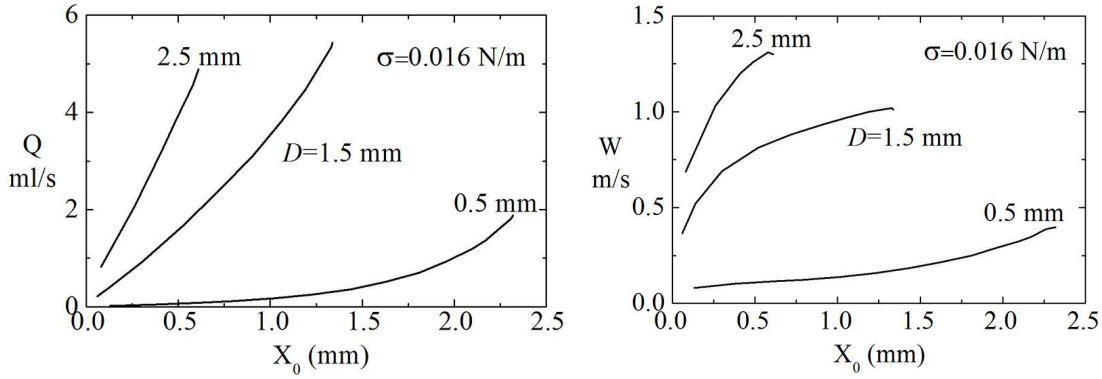

FIG. 9: (a) Flow rates of Freon R21 Q versus X_0 for the same values as in Fig. 8 ($\gamma = 7°$; $D = 0.5$, 1.5, and 2.5 mm; $R = 5$ mm), but for coefficient $\sigma = 0.016$ N/m and angle $\theta = 20°$; (b) averaged liquid velocities W versus X_0 for the same parameters as in (a)

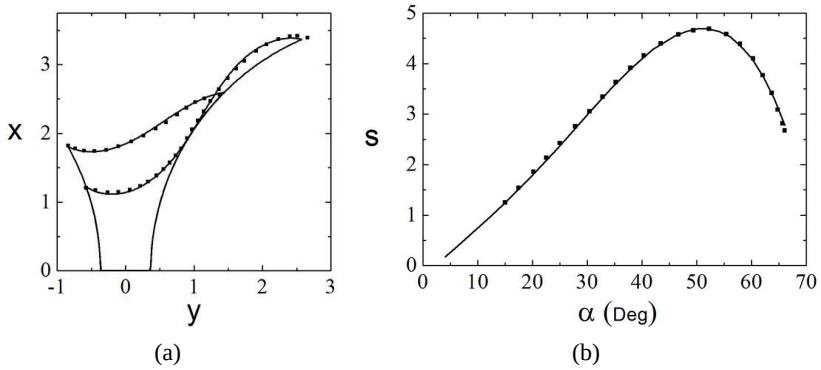

FIG. 10: Comparison of our calculations with the results obtained in Maltsev et al. (2016), shown by black squares: (a) two profiles of bridges; (b) area of bridge versus angle α (parameters: $r = 3.67$; $d = 0.734$; $\theta = 36°$)

We developed a simplified model with a narrow bridge between the cylinders (when $\alpha r \ll r$ and $\alpha \ll 1$). Let us integrate equation $\left(d^2w\right)/\left(dy^2\right) = -1$ by the bridge thickness and obtain for the velocity formula

$$w = \frac{y_\alpha^2 - y^2}{2} \tag{37}$$

where $y_\alpha = (d/2) + r\sin^2(\alpha/2)$ is the local semi-height of the bridge at point $x_\alpha = r\alpha$. The liquid flow rate is defined by the following formula:

$$q = r\int\limits_{-\alpha}^{\alpha} d\alpha \int\limits_{-y_\alpha}^{y_\alpha} w dy = \frac{r\alpha}{6}\left(d^3 + d^2 r\alpha^2 + \frac{3}{5}dr^2\alpha^4 + \frac{r^3\alpha^6}{7}\right) \tag{38}$$

The area of the bridge is

$$s = 4r\int\limits_0^{\alpha} y_\alpha d\alpha = 2r\alpha\left(d + \frac{r\alpha^2}{3}\right) \tag{39}$$

The average velocity of the liquid in the bridge is defined by expression

$$\bar{w} = \frac{q}{s} = \frac{\left[d^3 + d^2 r\alpha + (3/5)\, dr^2\alpha^4 + (1/7)\, r^3\alpha^6\right]}{12\left[d + r\,(\alpha^2/3)\right]} \tag{40}$$

It is interesting to look at these values in a limit of zero gap $d = 0$:

$$q = \frac{r^4\alpha^7}{6\cdot 7}, \quad s = \frac{2r^4\alpha^3}{3}, \quad \bar{w} = \frac{r^2\alpha^4}{28} \tag{41}$$

We have calculated the bridge area, flow rate, and averaged velocity of liquid for some examples and compared them with the simplified model in Figs. 11 and 12. Figures 11(a) and 11(b) show the calculated results for $r = 1$, $\theta = 10°$, and two distances $d = 0$ and 0.5. We see that for a small contact angle, the model deviation from the results obtained by the BEM is large. However, for large contact angle $\theta = 80°$, the simplified model gives good results, which are very close to the exact calculations, as demonstrated in Figs. 12(a) and 12(b).

5. CONCLUSIONS

A model of a liquid bridge formed in a gap between two cylinders, inclined to the horizon, was developed. Various shapes of the bridge free surface and forces acting on the cylinders were calculated. The forces can have different

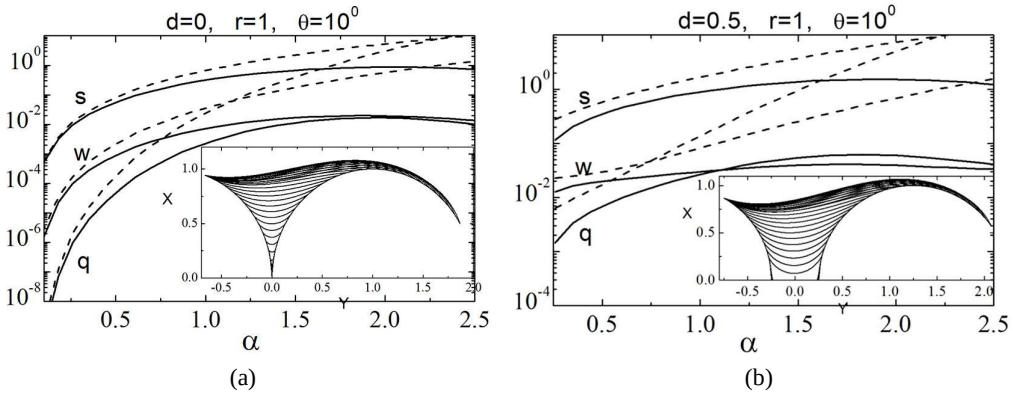

FIG. 11: Comparison of the results from the simplified model (dashed lines) with exact theory (solid lines): bridge area (s), flow rate (q), and averaged velocity of liquid (w), calculated for parameters $r = 1$ and $\theta = 10°$ at: (a) $d = 0$; (b) $d = 0.5$ (free surfaces of the bridges are shown in the insets)

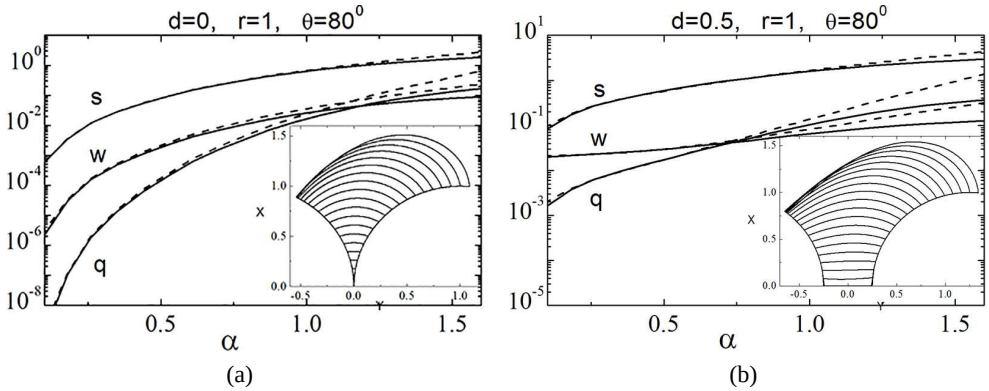

FIG. 12: Comparison of the simplified model (dashed lines) with exact theory (solid lines); curves are calculated for contact angle $\theta = 80°$ at: (a) $d = 0$; (b) $d = 0.5$ (free surfaces of the bridges are shown in the insets)

signs depending on the bridge shape, cylinder radius, contact angle, and gap size. The velocity field in the flowing bridge was determined by the BEM, based on the Navier–Stokes equation and reduced to the Laplace equation. The volumetric flow rate of the liquid in the inclined bridge was calculated. For the liquid flow in narrow gaps, an approximate model was constructed, and the results were in a good agreement with exact calculations by the BEM.

While considering real liquids (water and Freon R21), we have shown that the contact angle and surface tension affect the maximal width of the bridge but have little effect on the liquid flow in the bridge. The proposed size, X_0, which is the conditional half-width of the bridge measured along the midline of the bridge, is a convenient parameter for future measurements in experiments and for comparing calculated and experimental data.

In the four-dimensional parameter space, variants of bridges were calculated for a number of fixed values of the cylinder radius and contact angle in intervals $0.25 \leqslant r \leqslant 4$ and $0 \leqslant \theta \leqslant 90°$. For these variants, continuous dependences of the bridge characteristics on values d and α in intervals $0 \leqslant d \leqslant d_{\max}(r, \theta)$ and $0 \leqslant \alpha \leqslant \alpha_{\max}(r, \theta, d)$ were obtained, where values $d_{\max}$ and $\alpha_{\max}$ designate the limits of solution existence. We considered only cases of hydrophilic liquids ($\theta \leqslant 90°$), which are often used in engineering. Hydrophobic liquids ($\theta \geqslant 90°$) are found in natural phenomena, such as the movement of droplets and rivulets over lotus leaves. Such solutions are planned to be investigated in the future.

It is possible to show that heat exchange in an evaporating bridge is also described by the Laplace equation for the temperature field. Therefore, the method of boundary integral equations used here can be applied and heat transfer from the tubes to the vapor flow through the bridge body can be calculated. It is planned to describe this model in a subsequent article.

REFERENCES

Alekseenko, S.V., Geshev, P.I., and Kuibin, P.A., The Flow of Liquid with Free Boundary along Inclined Cylinder, *Rep. Acad. Sci. (Doklady)*, vol. **354**, no. 1, pp. 47–50, 1997.

Alekseenko, S.V. and Kuibin, P.A., Bridge Flow between Inclined Cylinders, *Proc. XXV Int. Siberian Seminar in Memory of S.S. Kutateladze*, Novosibirsk, Russia, pp. 19–31, 1996.

Brebbia, C.A., Telles, J.C.F., and Wrobel, L.C., *Boundary Element Techniques. Theory and Applications in Engineering*, Berlin, Germany: Springer-Verlag, 1984. DOI: 10.1007/978-3-642-48860-3

Buevich, Y.F. and Butkov, V.V., Regularities of Dispersion of Liquids with Slow Outflow from a Flat Gap, *Theor. Found. Chem. Technol*., vol. **3**, no. 4, pp. 576–582, 1969.

Kralchevsky, P.A. and Nagayama, K., Capillary Bridges and Capillary-Bridge Forces, in *Particles at Fluid Interfaces and Membranes*, D. Möbius and R. Miller, Eds., Amsterdam, Netherlands: Elsevier, chap. 11, pp. 469–502, 2001.

Landau, L.D. and Lifshits, E.M., *Fluid Mechanics*, Oxford, UK: Pergamon Press, 1987.

Maltsev, L.I., Houghton, P.A., and Kulikov, D.V., Bridge Flow of Liquid along a Gap between Inclined Cylinders, *Interf. Phenom. Heat Transf.*, vol. **4**, no. 4, pp. 269–277, 2016. DOI: 10.1615/InterfacPhenomHeatTransfer.2017021834

Maltsev, L.I. and Zuikova, V.I., About the Shape of Equilibrium Liquid Bridge between Two Horizontal Cylinders, *Thermophys. Aeromech*., vol. **11**, no. 1, pp. 115–120, 2004.

Myshkis, A.D., *Hydrodynamics of Weightlessness*, Moscow, USSR: Nauka, 1976.

Pitts, E., The Stability of Pendent Liquid Drops. Part 1. Drops Formed in Narrow Gap, *J. Fluid Mech*., vol. **59**, no. 4, pp. 753–767, 1973.

Reyssat, E., Capillary Bridges between a Plane and a Cylindrical Wall, *J. Fluid Mech*., vol. **773**, R1, pp. 1–12, 2015. DOI: 10.1017/jfm.2015.233

Tanasijczuk, A.J., Perazzo, C.A., and Gratton, J., Navier–Stokes Solutions for Steady-Sided Pendent Rivulets, *Eur. J. Mech. B Fluids*, vol. **29**, pp. 465–471, 2010. DOI: 10.1016/j.euromechflu.2010.06.002